Brazilian Journal of Medical and Biological Research (2015) 48(5): 408-414, http://dx.doi.org/10.1590/1414-431X20143962
ISSN 1414-431X

Sorafenib prevents liver fibrosis in a non-alcoholic steatohepatitis (NASH) rodent model

J.T. Stefano[1], I.V.A. Pereira[1], M.M. Torres[1], P.M. Bida[1], A.M.M. Coelho[2], M.P. Xerfan[1], B. Cogliati[4], D.F. Barbeiro[3], D.F.C. Mazo[1], M.S. Kubrusly[2], L.A.C. D'Albuquerque[2], H.P. Souza[3], F.J. Carrilho[1] and C.P. Oliveira[1]

[1]Disciplina de Gastroenterologia Clínica (LIM-07), Faculdade de Medicina, Universidade de São Paulo, São Paulo, SP, Brasil
[2]Disciplina de Transplante de Órgãos do Aparelho Digestivo (LIM-37), Faculdade de Medicina, Universidade de São Paulo, São Paulo, SP, Brasil
[3]Disciplina de Emergências Clínicas (LIM-51), Faculdade de Medicina, Universidade de São Paulo, São Paulo, SP, Brasil
[4]Departamento de Patologia, Faculdade de Medicina Veterinária e Zootecnia, Universidade de São Paulo, São Paulo, SP, Brasil

Abstract

Liver fibrosis occurring as an outcome of non-alcoholic steatohepatitis (NASH) can precede the development of cirrhosis. We investigated the effects of sorafenib in preventing liver fibrosis in a rodent model of NASH. Adult Sprague-Dawley rats were fed a choline-deficient high-fat diet and exposed to diethylnitrosamine for 6 weeks. The NASH group (n = 10) received vehicle and the sorafenib group (n = 10) received 2.5 $mg \cdot kg^{-1} \cdot day^{-1}$ by gavage. A control group (n = 4) received only standard diet and vehicle. Following treatment, animals were sacrificed and liver tissue was collected for histologic examination, mRNA isolation, and analysis of mitochondrial function. Genes related to fibrosis (*MMP9*, *TIMP1*, *TIMP2*), oxidative stress (*HSP60*, *HSP90*, *GST*), and mitochondrial biogenesis (*PGC1α*) were evaluated by real-time quantitative polymerase chain reaction (RT-qPCR). Liver mitochondrial oxidation activity was measured by a polarographic method, and cytokines by enzyme-linked immunosorbent assay (ELISA). Sorafenib treatment restored mitochondrial function and reduced collagen deposition by nearly 63% compared to the NASH group. Sorafenib upregulated *PGC1α* and *MMP9* and reduced *TIMP1* and *TIMP2* mRNA and IL-6 and IL-10 protein expression. There were no differences in *HSP60*, *HSP90* and *GST* expression. Sorafenib modulated *PGC1α* expression, improved mitochondrial respiration and prevented collagen deposition. It may, therefore, be useful in the treatment of liver fibrosis in NASH.

Key words: NASH; Fibrosis; Mitochondrial dysfunction; Sorafenib

Introduction

Liver cirrhosis represents a pathological response to chronic liver injury, regardless of etiology. Nonalcoholic fatty liver disease (NAFLD) encompasses a spectrum of liver diseases in which liver fibrosis can occur, usually preceding the development of cirrhosis and hepatocellular carcinoma (1).

The possibility of reversing hepatic fibrosis has prompted the investigation of promising antifibrotic therapies (2). Antifibrotic compounds are categorized by their mechanism of action, such as degradation of extracellular matrix, antioxidants, reduction of inflammation, and hepatic stellate cell (HSC) activation inhibitors, among others. Indeed, receptors including integrins, cytokines, growth factors such as transforming growth factor-β (TGF-β) and platelet-derived growth factor (PDGF), post-receptor signal regulators (Smads), and transcription factors such as peroxisome-proliferator-activated receptor gamma (PPAR-γ) have been suggested as potential targets for antifibrogenic therapeutic strategy (3,4).

Sorafenib is an antineoplastic drug that acts as a potent multikinase inhibitor of the vascular endothelial growth factor receptor (VEGFR), a PDGF receptor, and Raf, and has antitumor activity approved for the treatment of advanced renal cell carcinoma and hepatocellular carcinoma (HCC) (5,6). Sorafenib also has shown important antifibrotic effects on HSCs and liver endothelial cells. Experimental studies have found that sorafenib treatment reduced the number of activated HSCs (7), improved intrahepatic fibrosis, inflammation, and angiogenesis (8), and induced suppression of

Correspondence: C.P. Oliveira: <cpm@usp.br>.

Received March 25, 2014. Accepted November 12, 2014. First published online February 26, 2015.

collagen accumulation and HSC growth (9). Recently, Yang et al. (10) demonstrated that besides antifibrotic, antiangiogenic and portal hypertensive effects, chronic antagonism of anti-VEGFR improves hepatic blood flow, hepatic venous dysregulation, inhibits leukocyte recruitment/activation, splanchnic blood pooling and ascites formation in NASH-cirrhotic rats. However, the processes underlying these effects have not yet been fully characterized.

In this study, we evaluated the effects of sorafenib on liver fibrosis in an experimental model that used diethylnitrosamine (DEN) combined with a choline-deficient high-fat diet to induce NASH and liver fibrosis in Sprague-Dawley rats (11).

Material and Methods

Animals

Adult Sprague-Dawley rats weighing 250-300 g were housed in a temperature-, humidity-, and ventilation-controlled vivarium, with a 12-h light/dark cycle. All procedures for animal experimentation followed the ethical guidelines of the Helsinki Declaration of 1975 (NIH Publication No. 85-23, revised 1996) and the Guidelines of Animal Experimentation from the Faculdade de Medicina, Universidade de São Paulo.

Experimental procedures

NASH with fibrosis was induced in rats by a combination of a choline-deficient, high-fat diet (35% total fat, 54% trans fatty acid enriched; Rhoster Ltda., Brazil) and 13-15 mg/day diethylnitrosamine (DEN; Sigma Chemical, USA) administered in their drinking water (135 mg/L) as previously described (11) for 6 weeks. The animals were randomized to 3 treatment groups: NASH (n = 10), sorafenib (n = 10), and control (n = 4). Animals in both the NASH and sorafenib groups received the study diet and DEN; sorafenib group animals received 2.5 $mg \cdot kg^{-1} \cdot day^{-1}$ sorafenib and NASH animals received vehicle (Ringer's solution) daily by gavage. Control animals were fed *ad libitum* with a standard diet (Nuvilab® Nutrientes Ltda., Brazil), and received Ringer's solution by gavage. Dietary intake was assessed by weighing the amount eaten every 3 days. After the 6-week period, the animals were anesthetized with 0.1 mL/kg intraperitoneal ketamine and sacrificed. Liver specimens were obtained for histopathological, gene expression, cytokine, and liver mitochondrial function analyses.

Histological analysis

After initial gross evaluation, liver tissue samples were fixed in 4% formaldehyde and processed for hematoxylin-eosin and picrosirius staining for histological analysis. Collagen content was determined by light microscopy (Nikon E-800, Japan) in picrosirius-stained histological sections. Since the distribution of injuries in the samples was heterogeneous and different damage patterns were observed, quantification was performed in areas with greater collagen deposition. The analysis was standardized for all animals and conducted in a blinded manner. Ten histological fields per sample were studied (total area of 3,031,614 μm^2). The collagen fiber area was quantified with Image Pro-Plus 4.5 (Media Cybernetics Inc., USA), as described elsewhere (12). The results are reported as the percentage of the area occupied by collagen in relation to the total histological field.

Gene expression analysis

Tissue RNA extraction was performed by the Trizol® method and quantification of total extracted RNA was determined by spectrophotometry (Nanodrop ND-1000; Nanodrop Technologies, USA). The RNA preparation was considered free of proteins when the $absorbance_{260/280}$ ratio was between 1.8 and 2.0. Real-time quantitative polymerase chain reaction (RT-qPCR) protocols were performed with a Rotor-Gene RG-3000 thermal cycler (Corbett Research, Australia) and SuperScript™ III Platinum® One-Step Quantitative RT-PCR System reagents (Invitrogen Life Technologies, USA) as recommended by the manufacturers. All RT-qPCR reactions were performed in duplicate for each sample of liver tissue for both the target gene and the *β-actin* control. The primers for the *TIMP1*, *TIMP2*, *MMP9*, *HSP60*, *HSP90*, *GST*, *PGC1α*, and *β-actin* genes were designed in the Primer3 Input program (http://frodo.wi.mit.edu/). The *β-actin* gene was used as the endogenous control. Relative quantification was calculated using the mathematical model described by Pfaffl (13). The primer sequences for each gene were as follows: *HSP-60* forward, AGC AAA GGG GCT AAT CCA GT and reverse, TGA CAC CCT TTC TTC CAA CC; *HSP-90* forward, GAT TGA CAT CAT CCC CAA CC and reverse, CTG CTC ATC ATC GTT GTG CT; *GST* forward, GGC GGA TCT GGA TGA AAT AGT TCT and reverse, CAA CGA GAT AAT CTT GTC CAT GGC; *TIMP1*, forward, TCC CCA GAA ATC ATC GAG AC and reverse, TCA GAT TAT GCC AGG GAA CC; *TIMP2* forward, GCA TCA CCC AGA AGA AGA GC and reverse, GGG TCC TCG ATG TCA AGA AA; *MMP-9* forward, CAA ACC CTG CGT ATT TCC AT and reverse, AGA GTA CTG CTT GCC CAG GA; *PGC1α* forward, CTA CAG ACA CCG CAC ACA TCG C and reverse, TCT CTC TGC TTG GCC CTT TCA G; *β-actin* forward, TGT CAC CAA CTG GGA CGA TA and reverse, GGG GTG TTG AAG GTC TCA AA; *GAPDH* forward, ATG ATT CTA CCC ACG GCA AG and reverse, CTG GAA GAT GGT GAT GGG TT.

Liver mitochondrial oxidation and phosphorylation activities

Liver mitochondria were prepared as previously described (14). The mitochondrial oxygen consumption was measured polarographically using a Gilson 5/6H Oxygraph (Gilson Medical Electronics, Inc., USA) at 28°C in a closed reaction vessel fitted with a Clark oxygen electrode (Yellow Springs Instruments Co., USA). The incubation medium consisted of 120 mM KCl, 2 mM sodium phosphate, 10 μM rotenone, and 1 mM EGTA (ethylene glycol-bis

(2-aminoethylether)-N,N,N′,N′-tetraacetic acid) and was buffered at pH 7.3 with 5 mM Tris-HCl. Mitochondria were energized with potassium succinate as substrate at a final concentration of 10 mM. After a brief equilibration period, state 3 (activated state, S3) respiration was induced by the addition of 280 nmol adenosine diphosphate (ADP). The added ADP was phosphorylated to adenosine triphosphate (ATP) and the state 4 (basal state, S4) respiration was then measured. The ratio of oxygen consumption in the presence of ADP to that in the absence (respiratory control rate, RCR) and the ADP/O ratio was calculated as an index of mitochondrial oxidation and phosphorylation. RCR was calculated as oxygen consumption in S3/oxygen consumption in S4; ADP/O as moles of ATP formed from ADP per atom of oxygen consumed. S3 and S4 are reported as nanomoles of oxygen per milligram mitochondrial protein per minute ($nmol.mg^{-1}.min^{-1}$). Mitochondrial protein content was determined by the Lowry method (15).

Cytokine analysis

For the determination of cytokine levels, the liver tissue samples were ground in ice-cold radio-immunoprecipitation assay buffer. TNF-α, IL-6, and IL-10 were measured in each of the liver samples by enzyme-linked immunosorbent assay (ELISA) (R&D System Inc., USA), in accordance with the manufacturer's instructions (16). All measurements were made in duplicate, and the average values were used in the statistical analyses.

Statistical analysis

Data are reported as means with 95% confidence intervals (CIs). All analyses were performed with the statistical computing package R (version 2.15.2; The R Project for Statistical Computing, http://www.r-project.org). The Shapiro-Wilk normality test and Levene's variance homogeneity test were applied to verify normality and homogeneity of variance. Analysis of variance (ANOVA) followed by Tukey's *post hoc* test was used to identify statistical differences in homogeneous, normally distributed data. The Kruskal-Wallis non-parametric test was used to analyze data not normally distributed or homogeneous. Significance was set at $P<0.05$.

Results

Sorafenib prevented NASH-related fibrosis

Histochemical analyses were performed to evaluate the degree of fibrosis in our NASH experimental model, as previously described. We observed a marked increase in mean collagen content in animals fed a choline-deficient high-fat diet plus DEN (7.35; 95%CI: 4.84-9.85) compared to control rats (0.52; 95%CI: 0.45-0.57) ($P<0.001$), indicating the effectiveness of this model in inducing early stages of fibrosis. Interestingly, sorafenib treatment reduced collagen content (3.41; 95%CI: 2.53-4.28) compared with the NASH group ($P<0.001$) (Figure 1). To understand the mechanisms underlying the latter effect, we investigated the processes associated with collagen production and degradation. No difference was observed in mean *MMP9* mRNA transcription level in liver tissue from NASH (0.99; 95%CI: 0.90-1.07) compared to control rats (1.00; 95%CI: 0.95-1.07; $P=0.834$). However, mean *MMP9* mRNA content was significantly increased in animals treated with sorafenib (1.61; 95%CI: 1.35-1.86) compared to both the control and NASH groups ($P<0.001$, Figure 2C). We observed that mean mRNA expression of *TIMP1*, an *MMP9* inhibitor, was significantly lower in NASH animals (0.87; 95%CI: 0.80-0.94) than in controls (1.00; 95%CI: 0.96-1.04, $P=0.036$) and further impaired in sorafenib-treated rats (0.74; 95%CI: 0.68–0.81; $P<0.001$ *vs* controls and $P=0.015$ *vs* NASH;

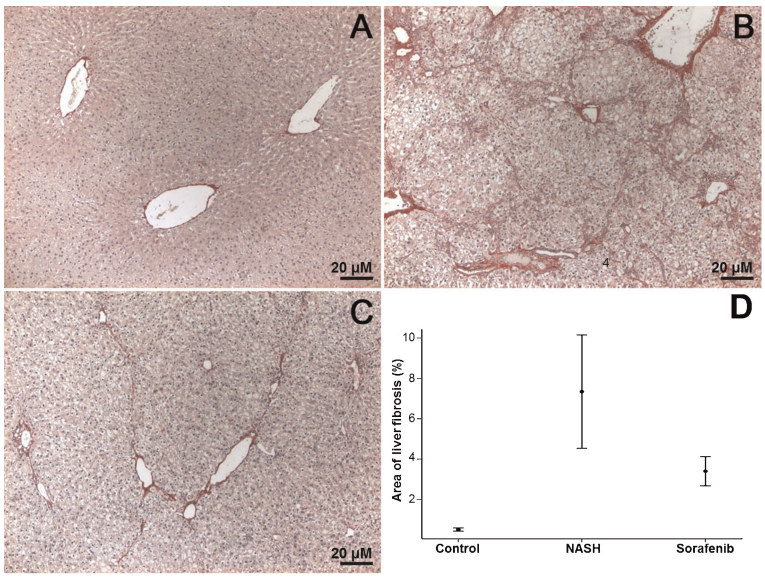

Figure 1. Analysis of liver extracellular matrix by morphometry of collagen fibers stained in red with Sirius Red. *A*, Control animal (n = 4); *B*, nonalcoholic steatohepatitis (NASH) animal that received only vehicle (n = 10); *C*, NASH animal treated with 2.5 $mg \cdot kg^{-1} \cdot day^{-1}$ of sorafenib for 6 weeks (n = 10); *D*, graph demonstrating that NASH animals treated with sorafenib presented a decrease in the area occupied by collagen fibers in liver parenchyma compared with NASH animals that received only vehicle ($P<0.001$, Tukey test).

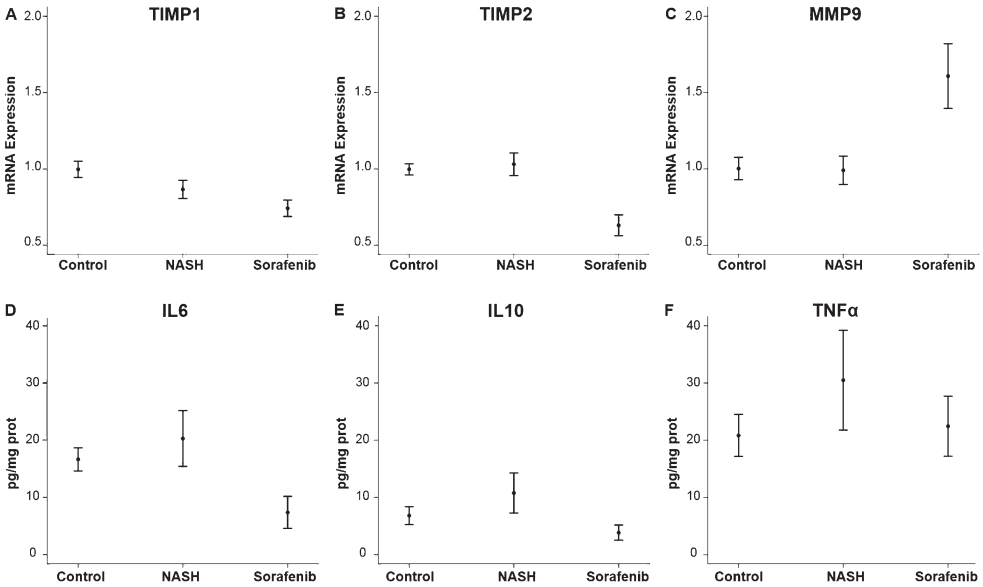

Figure 2. *A*, *B*, *C*, Graphic representation of *TIMP1*, *TIMP2*, and *MMP9* mRNA expression in control (n = 4), nonalcoholic steatohepatitis (NASH; n = 10), and sorafenib-treated animals (n = 10). *A*, *TIMP1* mRNA expression was significantly lower in NASH animals compared to control (P = 0.036, Tukey test) and further impaired in sorafenib-treated rats (P<0.001 *vs* control and P = 0.015 *vs* NASH, Tukey test). *B*, *TIMP2* was significantly lower in the sorafenib group compared to control and NASH groups (P<0.001, Tukey test). *C*, *MMP9* mRNA content was increased in animals treated with sorafenib (P<0.001 *vs* control and NASH, non-parametric Tukey test). There was no statistical difference in *MMP9* mRNA transcription levels in the liver from NASH animals compared to control rats (P = 0.834, non-parametric Tukey test). *D*, *E*, *F*, Graphic representation of IL-6, IL-10, and TNF-α in control, NASH, and sorafenib-treated animals. *D*, Protein levels of IL-6 were similar in the NASH and control groups (P = 0.55, Tukey test). IL-6 levels were significantly lower in sorafenib animals compared to NASH animals (P = 0.002, Tukey test). *E*, IL-10 protein levels were also lower in the sorafenib group compared to the NASH (P<0.001, non-parametric Tukey test) and control groups (P = 0.039, non-parametric Tukey test). *F*, No differences in TNF-α protein levels were detected among the three groups (non-parametric Tukey test).

Figure 2A). The expression of *TIMP2* was significantly lower in the sorafenib group (0.63; 95%CI: 0.55-0.71) than in controls (1.00; 95%CI: 0.97-1.03) and the NASH group (1.03; 95%CI: 0.94-1.12; both P<0.001; Figure 2B). Together these data suggest that collagen degradation was enhanced by treatment with sorafenib, resulting in less fibrosis.

Anti-inflammatory effect of sorafenib on NASH-related fibrosis

Treatment with sorafenib was associated with a significant decrease in IL-6 and IL-10 protein expression, suggesting that it may indeed have a mild anti-inflammatory effect. Levels of IL-6 protein in the NASH group (20.30; 95%CI: 14.56-26.04) and control group (16.66; 95%CI: 14.89-18.44) did not differ (P = 0.55). IL-6 levels were significantly lower in the sorafenib group (7.39; 95%CI: 4.68-9.75) than in the NASH group (P = 0.002). IL-10 protein levels were also lower in the sorafenib group (3.86; 95%CI: 2.71-5.00) than in both the NASH (10.78; 95%CI: 7.49-13.59; P<0.001) and control (6.84; 95%CI: 5.46; 8.14; P = 0.039) groups. No differences in TNF-α protein levels were detected among the 3 groups (Figure 2D,E,F).

Redox signaling in NASH was not the main target for sorafenib

No differences were observed in hepatic heat shock protein expression. Mean *HSP60* expression was 1.00 (95%CI: 0.95-1.07) for controls, 0.98 (95%CI: 0.95-1.02) for the NASH group, and 0.95 (95%CI: 0.92-0.97) for the sorafenib group. The corresponding values for *HSP90* were 1.00 (95%CI: 0.97-1.03) for controls, 1.03 (95%CI: 1.00-1.05) for the NASH group, and 1.06 (95%CI: 1.02-1.09) for the sorafinib group. No differences were observed in the expression of *GST*, an enzyme responsible for maintaining glutathione homeostasis and the main intracellular redox buffer. The values were 1.00 (95%CI: 0.99-1.02) for controls, 0.99 (95%CI: 0.97-1.02) for the NASH group, and 0.92 (95%CI: 0.86-0.98) for the sorafenib group (Figure 3A,B,C).

Sorafenib prevented mitochondrial dysfunction in NASH

As shown in Figure 4A, all stages of mitochondrial respiration in liver homogenates from NASH animals were markedly impaired compared to controls. Sorafenib treatment was associated with a significant improvement in mitochondrial function at all stages, restoring all parameters

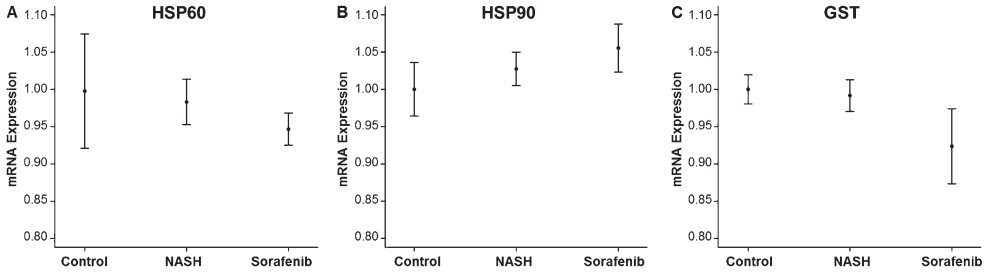

Figure 3. Graphic representation of *HSP60*, *HSP90*, and *GST* mRNA expression in control (n = 4), nonalcoholic steatohepatitis (NASH; n = 10), and sorafenib-treated animals (n = 10). The mRNA expression of *HSP60*, *HSP90*, and *GST* did not differ among the three groups.

to almost the levels observed in control animals. Figure 4B shows that mean *PGC1α* mRNA levels were markedly lower in NASH subjects (0.40; 95%CI: 0.30-0.50) than in controls ($P<0.001$), but the control (1.00; 95%CI: 0.70-1.27) and the sorafenib (1.24; 95%CI: 0.71-1.69) groups were not significantly different ($P = 0.99$). Mean *PGC1α* mRNA expression in the NASH group was significantly lower than in the sorafenib group; $P<0.001$). These results point strongly to the potent effect of sorafenib in correcting mitochondrial dysfunction, mainly by enhancing *PGC1α* expression.

A

	RCR	S3	S4
CTRL	3.09 ± 0.03	77.27 ± 4.80	25.42 ± 1.47
NASH	1.86 ± 0.07*	32.55 ± 3.23*	17.52 ± 1.22*
Sorafenib	2.64 ± 0.13#	59.93 ± 4.42#	22.75 ± 1.27#

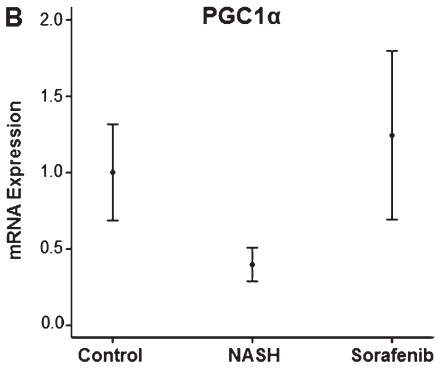

Figure 4. *A*, Stages of mitochondrial respiration in liver homogenates of control (CTRL; n = 4), nonalcoholic steatohepatitis (NASH; n = 10), and sorafenib-treated animals (n = 10). All stages of mitochondrial respiration in liver homogenates from NASH animals were markedly impaired compared to controls. Sorafenib treatment improved mitochondrial function, restoring the parameters to almost the levels observed in control animals. RCR: respiratory control rate; S3: activated state; S4: basal state respiration. *$P<0.05$ compared to CTRL group; #$P<0.05$ compared to NASH group (Tukey test). *B*, Graphic representation of *PGC1α* mRNA expression in control, NASH, and sorafenib-treated animals ($P = 0.99$, control *vs* sorafenib group; $P<0.001$, control *vs* NASH; $P<0.001$, NASH *vs* sorafenib group; non-parametric Tukey test).

Discussion

This study showed that the antineoplastic drug sorafenib prevented the early stages of fibrosis in an experimental model of NASH. Sorafenib was shown not only to have mild anti-inflammatory properties, but also to prevent the mitochondrial dysfunction that characterizes this condition.

Treatment with sorafenib reduced collagen deposition by nearly 63% in this model. These data corroborate previous results by Hong et al. (17) that also demonstrated a greater than 60% reduction in collagen deposition in animals treated with sorafenib. Further investigation revealed that increased expression of *MMP9* together with lower levels of *TIMP1* and *TIMP2* is crucial for matrix remodeling, despite possessing no activity against type I collagen (18). It may, however, exert an indirect effect on fibrosis resolution, since increased *MMP9* activity markedly accelerates the onset of fibrinolysis (18-20). It has also been suggested that *MMP9* accelerates apoptosis of HSCs, thereby contributing to fibrosis regression (21). In this context, our findings are the first to show an effect of sorafenib on *MMP9* gene expression, thus uncovering a new mechanism whereby this drug may affect liver fibrosis.

MMP9 gene expression and protein activity are tightly regulated, being induced by reactive oxygen species and inflammatory mediators. Therefore, we sought further to determine whether the observed increase in *MMP9* expression resulted from changes in those signaling pathways.

Since inflammatory cytokines play a key role in fibrogenesis, and persistent inflammation always precedes liver fibrosis and its progression to more severe forms (22,23), our data suggest that lower IL-6 and IL-10 levels were present in sorafenib-treated than in NASH rats, suggesting that the beneficial effect of sorafenib may be at least partially due to its anti-inflammatory activity.

Mitochondria play a central role in fat oxidation and cellular energy metabolism, being responsible for oxidative phosphorylation and fatty acid β-oxidation (24). Indeed, various changes in mitochondrial metabolism have been

implicated in NASH pathogenesis and carcinogenesis, secondary to their role in pathways associated with cellular energy metabolism, free radical generation, and apoptosis (25-32). In NASH, mitochondrial dysfunction has been associated with the development, perpetuation, and worsening of the disease (26). The loss of mitochondrial function leads to the accumulation of lipid deposits in the cytosol and participates at various levels in NASH pathogenesis. It not only impairs fat metabolism but also increases oxidative stress and cytokine production, triggering cell death, inflammation, and fibrosis (33,34). We report here that mitochondrial respiration is severely impaired in NASH. All steps of the respiratory chain are affected, suggesting a global mitochondrial dysfunction. We demonstrated here, as in a previous study from our group (35), a significant reduction in RCR in the NASH group, suggesting mitochondrial dysfunction. Moreover, we observed a recovery of RCR, similar to the control group, in the animals treated with sorafenib. However, we cannot exclude interference by sorafenib in mitochondrial biogenesis, which differs in tissues depending on the numbers of mitochondria, and the participation of other cells, such as fibroblasts, to explain this finding.

The transcriptional coactivator PPAR-γ coactivator-1 (PGC-1) is a main regulator of mitochondrial function and biogenesis. PGC-1 interacts with peroxisome proliferator-activated receptor alpha (PPAR-α) to increase mitochondrial β-oxidation of fatty acids, increasing the expression of nuclear respiratory factor-1 and mitochondrial transcription factor A, which in turn increase the number of mitochondria and their oxidative phosphorylation capacity (36). Based on these findings, we examined whether *PGC1*α was involved in this process. *PGC1*α is the main regulator of mitochondrial biogenesis and oxidative phosphorylation. It is highly expressed in the liver, and its expression may be modulated by physiological and pathological stimuli. We observed that *PGC1*α expression decreased during NASH development, reaching a nadir when fibrosis was fully present. Interestingly, both *PGC1*α expression and mitochondrial respiration were restored by treatment with sorafenib. However, although these results suggest that sorafenib modulates *PGC1*α expression, improves mitochondrial respiration, and prevents collagen deposition, our data do not support these as the primary actions of sorafenib. We do not know how sorafenib affects *PGC1*α expression, which leads to improvement of mitochondrial respiration. Further studies are needed to clarify the exact role of sorafenib in the enhanced *PGC1*α expression and in the global improvement in mitochondrial respiration.

In summary, we have shown that liver fibrosis after NASH development is characterized by enhanced collagen deposition and *MMP-9* activity. These findings were not clearly related to imbalances in redox signaling or inflammatory mediators. Metabolic abnormalities, characterized by mitochondrial dysfunction and impaired *PGC1*α expression, were seen in this experimental model and were corrected by sorafenib treatment. Sorafenib, by preventing mitochondrial dysfunction, may contribute to the treatment of not only liver diseases but also of other metabolic and degenerative diseases.

Acknowledgments

We wish to thank Bayer® HealthCare Pharmaceuticals for providing sorafenib, and the Alves de Queiroz Family Fund for Research and CNPq for financial support.

References

1. Vernon G, Baranova A, Younossi ZM. Systematic review: the epidemiology and natural history of non-alcoholic fatty liver disease and non-alcoholic steatohepatitis in adults. *Aliment Pharmacol Ther* 2011; 34: 274-285, doi: 10.1111/j.1365-2036.2011.04724.x.
2. Bonis PA, Friedman SL, Kaplan MM. Is liver fibrosis reversible? *N Engl J Med* 2001; 344: 452-454, doi: 10.1056/NEJM200102083440610.
3. Bataller R, Sancho-Bru P, Gines P, Brenner DA. Liver fibrogenesis: a new role for the renin-angiotensin system. *Antioxid Redox Signal* 2005; 7: 1346-1355, doi: 10.1089/ars.2005.7.1346.
4. Ahmad A, Ahmad R. Understanding the mechanism of hepatic fibrosis and potential therapeutic approaches. *Saudi J Gastroenterol* 2012; 18: 155-167, doi: 10.4103/1319-3767.96445.
5. Escudier B, Eisen T, Stadler WM, Szczylik C, Oudard S, Siebels M, et al. Sorafenib in advanced clear-cell renal-cell carcinoma. *N Engl J Med* 2007; 356: 125-134, doi: 10.1056/NEJMoa060655.
6. Llovet JM, Ricci S, Mazzaferro V, Hilgard P, Gane E, Blanc JF, et al. Sorafenib in advanced hepatocellular carcinoma. *N Engl J Med* 2008; 359: 378-390, doi: 10.1056/NEJMoa0708857.
7. Hennenberg M, Trebicka J, Kohistani Z, Stark C, Nischalke HD, Kramer B, et al. Hepatic and HSC-specific sorafenib effects in rats with established secondary biliary cirrhosis. *Lab Invest* 2011; 91: 241-251, doi: 10.1038/labinvest.2010.148.
8. Mejias M, Garcia-Pras E, Tiani C, Miquel R, Bosch J, Fernandez M. Beneficial effects of sorafenib on splanchnic, intrahepatic, and portocollateral circulations in portal hypertensive and cirrhotic rats. *Hepatology* 2009; 49: 1245-1256, doi: 10.1002/hep.22758.
9. Wang Y, Gao J, Zhang D, Zhang J, Ma J, Jiang H. New insights into the antifibrotic effects of sorafenib on hepatic stellate cells and liver fibrosis. *J Hepatol* 2010; 53: 132-144, doi: 10.1016/j.jhep.2010.02.027.
10. Yang YY, Liu RS, Lee PC, Yeh YC, Huang YT, Lee WP, et al. Anti-VEGFR agents ameliorate hepatic venous dysregulation/microcirculatory dysfunction, splanchnic venous pooling and ascites of NASH-cirrhotic rat. *Liver Int* 2014; 34: 521-534, doi: 10.1111/liv.12299.
11. de Lima V, Oliveira CP, Alves VA, Chammas MC, Oliveira EP,

Stefano JT, et al. A rodent model of NASH with cirrhosis, oval cell proliferation and hepatocellular carcinoma. *J Hepatol* 2008; 49: 1055-1061, doi: 10.1016/j.jhep.2008.07.024.
12. Cogliati B, Pereira HM, Dagli ML, Parra OM, Silva JR, Hernandez-Blazquez FJ. Hepatotrophic factors reduce hepatic fibrosis in rats. *Arq Gastroenterol* 2010; 47: 79-85.
13. Pfaffl MW. A new mathematical model for relative quantification in real-time RT-PCR. *Nucleic Acids Res* 2001; 29: e45, doi: 10.1093/nar/29.9.e45.
14. Coelho AM, Machado MC, Sampietre SN, Leite KR, Molan NA, Pinotti HW. [Hepatic lesion in experimental acute pancreatitis. Influence of pancreatic enzyme storage reduction]. *Rev Hosp Clin Fac Med São Paulo* 1998; 53: 104-109.
15. Lowry OH, Rosebrough NJ, Farr AL, Randall RJ. Protein measurement with the Folin phenol reagent. *J Biol Chem* 1951; 193: 265-275.
16. Soriano FG, Liaudet L, Szabo E, Virag L, Mabley JG, Pacher P, et al. Resistance to acute septic peritonitis in poly(ADP-ribose) polymerase-1-deficient mice. *Shock* 2002; 17: 286-292, doi: 10.1097/00024382-200204000-00008.
17. Hong F, Chou H, Fiel MI, Friedman SL. Antifibrotic activity of sorafenib in experimental hepatic fibrosis: refinement of inhibitory targets, dosing, and window of efficacy *in vivo*. *Dig Dis Sci* 2013; 58: 257-264, doi: 10.1007/s10620-012-2314-1.
18. Hemmann S, Graf J, Roderfeld M, Roeb E. Expression of MMPs and TIMPs in liver fibrosis - a systematic review with special emphasis on anti-fibrotic strategies. *J Hepatol* 2007; 46: 955-975, doi: 10.1016/j.jhep.2007.02.003.
19. Ueberham E, Low R, Ueberham U, Schonig K, Bujard H, Gebhardt R. Conditional tetracycline-regulated expression of TGF-beta1 in liver of transgenic mice leads to reversible intermediary fibrosis. *Hepatology* 2003; 37: 1067-1078, doi: 10.1053/jhep.2003.50196.
20. Roderfeld M, Hemmann S, Roeb E. Mechanisms of fibrinolysis in chronic liver injury (with special emphasis on MMPs and TIMPs). *Z Gastroenterol* 2007; 45: 25-33, doi: 10.1055/s-2006-927388.
21. Roderfeld M, Weiskirchen R, Wagner S, Berres ML, Henkel C, Grotzinger J, et al. Inhibition of hepatic fibrogenesis by matrix metalloproteinase-9 mutants in mice. *FASEB J* 2006; 20: 444-454, doi: 10.1096/fj.05-4828com.
22. Das SK, Balakrishnan V. Role of cytokines in the pathogenesis of non-alcoholic Fatty liver disease. *Indian J Clin Biochem* 2011; 26: 202-209, doi: 10.1007/s12291-011-0121-7.
23. Coulon S, Francque S, Colle I, Verrijken A, Blomme B, Heindryckx F, et al. Evaluation of inflammatory and angiogenic factors in patients with non-alcoholic fatty liver disease. *Cytokine* 2012; 59: 442-449, doi: 10.1016/j.cyto.2012.05.001.
24. Fromenty B, Grimbert S, Mansouri A, Beaugrand M, Erlinger S, Rotig A, et al. Hepatic mitochondrial DNA deletion in alcoholics: association with microvesicular steatosis. *Gastroenterology* 1995; 108: 193-200, doi: 10.1016/0016-5085(95)90024-1.
25. Sanyal AJ. Nonalcoholic fatty liver disease in the Indian subcontinent: a medical consequence of globalization? *Indian J Gastroenterol* 2001; 20: 215-216.
26. Begriche K, Igoudjil A, Pessayre D, Fromenty B. Mitochondrial dysfunction in NASH: causes, consequences and possible means to prevent it. *Mitochondrion* 2006; 6: 1-28, doi: 10.1016/j.mito.2005.10.004.
27. Serviddio G, Sastre J, Bellanti F, Vina J, Vendemiale G, Altomare E. Mitochondrial involvement in non-alcoholic steatohepatitis. *Mol Aspects Med* 2008; 29: 22-35, doi: 10.1016/j.mam.2007.09.014.
28. Caldwell SH, Swerdlow RH, Khan EM, Iezzoni JC, Hespenheide EE, Parks JK, et al. Mitochondrial abnormalities in non-alcoholic steatohepatitis. *J Hepatol* 1999; 31: 430-434, doi: 10.1016/S0168-8278(99)80033-6.
29. Cortez-Pinto H, Chatham J, Chacko VP, Arnold C, Rashid A, Diehl AM. Alterations in liver ATP homeostasis in human nonalcoholic steatohepatitis: a pilot study. *JAMA* 1999; 282: 1659-1664, doi: 10.1001/jama.282.17.1659.
30. Perez-Carreras M, Del Hoyo P, Martin MA, Rubio JC, Martin A, Castellano G, et al. Defective hepatic mitochondrial respiratory chain in patients with nonalcoholic steatohepatitis. *Hepatology* 2003; 38: 999-1007, doi: 10.1053/jhep.2003.50398.
31. Pessayre D. Role of mitochondria in non-alcoholic fatty liver disease. *J Gastroenterol Hepatol* 2007; 22 (Suppl 1): S20-S27, doi: 10.1111/j.1440-1746.2006.04640.x.
32. Serviddio G, Bellanti F, Vendemiale G, Altomare E. Mitochondrial dysfunction in nonalcoholic steatohepatitis. *Expert Rev Gastroenterol Hepatol* 2011; 5: 233-244, doi: 10.1586/egh.11.11.
33. Grattagliano I, Caraceni P, Calamita G, Ferri D, Gargano I, Palasciano G, et al. Severe liver steatosis correlates with nitrosative and oxidative stress in rats. *Eur J Clin Invest* 2008; 38: 523-530, doi: 10.1111/j.1365-2362.2008.01963.x.
34. Rolo AP, Teodoro JS, Palmeira CM. Role of oxidative stress in the pathogenesis of nonalcoholic steatohepatitis. *Free Radic Biol Med* 2012; 52: 59-69, doi: 10.1016/j.freeradbiomed.2011.10.003.
35. Oliveira CP, Coelho AM, Barbeiro HV, Lima VM, Soriano F, Ribeiro C, et al. Liver mitochondrial dysfunction and oxidative stress in the pathogenesis of experimental nonalcoholic fatty liver disease. *Braz J Med Biol Res* 2006; 39: 189-194, doi: 10.1590/S0100-879X2006000200004.
36. Vega RB, Huss JM, Kelly DP. The coactivator PGC-1 cooperates with peroxisome proliferator-activated receptor alpha in transcriptional control of nuclear genes encoding mitochondrial fatty acid oxidation enzymes. *Mol Cell Biol* 2000; 20: 1868-1876, doi: 10.1128/MCB.20.5.1868-1876.2000.